

## Dissolution processes, hydrolysis and condensation reactions during geopolymer synthesis: Part I—Low Si/Al ratio systems

L. Weng · K. Sagoe-Crentsil

Received: 29 August 2005 / Accepted: 18 August 2006 / Published online: 9 January 2007  
© Springer Science+Business Media, LLC 2007

**Abstract** Initial geopolymeric reaction processes governing dissolution of solid aluminosilicate particles in alkali solutions have been investigated using conventional experimental techniques, and the data analysed by speciation predictions of the partial charge model (PCM). For metakaolin powders activated with 5.0 M NaOH, solid-state nuclear magnetic resonance (NMR) spectra disclose the existence of monomeric  $[\text{Al}(\text{OH})_4]^-$  species after two hours of dissolution, consistent with PCM predictions. However, no equivalent monomeric silicate species were observed for 5.0–10.0 M NaOH activator solutions characteristic of systems with nominal  $\text{Si}/\text{Al} \leq 1$ . The apparent absence of monomeric silicate species suggest rapid condensation of silicate units with  $[\text{Al}(\text{OH})_4]^-$  to generate aluminosilicate species, as indicated by the evolution of the shoulder at around  $-87$  ppm in the  $^{29}\text{Si}$  NMR spectra. Of the two possible stable silicate species  $[\text{SiO}_2(\text{OH})_2]^{2-}$  and  $[\text{SiO}(\text{OH})_3]^-$ , the latter appears most likely to condense with  $[\text{Al}(\text{OH})_4]^-$  to produce aluminosilicate oligomers, from which larger oligomers subsequently form through further condensation with  $[\text{Al}(\text{OH})_4]^-$  leading to a gradual build up of aluminosilicate networks and a lowering of system alkalinity. This dissolution and hydrolysis sequence at the early stages of synthesis suggests a reaction path wholly consistent with predictions of the partial charge model.

### Introduction

Geopolymer systems composed of alkaline aluminosilicates have generated strong interest due to their potentially remarkable mechanical properties, excellent fire performance and good acid resistivity [1]. During the last two decades, several international conferences have been held on these systems covering formation mechanisms, processing, properties and applications of these materials [2–4]. The optimal compositions of geopolymers were initially given by Davidovits et al. [5], with typical nominal molar ratios of Si/Al 1, 2 and 3, and respectively named poly(sialate), poly(sialate-siloxo) and poly(sialate-disiloxo). Nuclear magnetic resonance (NMR) evidence [5, 6] showed that both Al and Si atoms in geopolymers are 4-coordinated and form tetrahedra, which connect to each other by corner-sharing oxygen atoms. Although  $[\text{AlO}_4]$  tetrahedra generally avoid links between themselves, as stated by Lowenstein's rule [7], recent studies [8] indicate the linkage of Al–O–Al is possible, specially under lower silicate conditions. The microstructure and porosity of this class of materials were studied by Palomo and Glasser [9], and the relationship between the composition and mechanical properties of geopolymers were researched by Steveson and Sagoe-Crentsil [10] and Davidovits [11]. These researchers noted that geopolymers are different in chemical composition from alkaline-activated cement, having a characteristic calcium silicate hydrate (C–S–H) gel phase as opposed to the amorphous aluminosilicate phase characteristic of geopolymers. These compositional and microstructural differences exist, probably from the micrometer level down to nanometer scale. However, low curing

L. Weng  
Department of Materials Science, Shenzhen Graduate  
School, Harbin Institute of Technology, University Town,  
Xili, Shenzhen 518055, P.R. China

K. Sagoe-Crentsil (✉)  
Manufacturing & Infrastructure Technology, CSIRO,  
P.O. Box 56, Highett, Victoria 3190, Australia  
e-mail: Kwesi.Sagoe-Crentsil@csiro.au

temperatures, processing conditions and, in most cases, applications are common to both cements and geopolymers.

Although geopolymers have similar chemical constituents to zeolites, they generally differ from crystalline zeolites with respect to precursor material processing and applications. Therefore, geopolymers need to be regarded as a unique class of materials.

Essentially the synthesis of geopolymers involves the dissolution of mineral aluminosilicates, hydrolysis of  $\text{Al}^{3+}$  and  $\text{Si}^{4+}$  components, and condensation of specific aluminate and silicate species. There are several published experimental research reports [12–14] on the formation, properties and applications of geopolymer materials, but the theoretical study on the mechanism of formation of geopolymers is only now emerging [8].

Our previous work [15] showed that Livage's partial charge model [16] is applicable to the investigation of the hydrolysis and condensation of alkaline silicates in solutions. Although the condensation between aluminates and silicates was also briefly discussed in that work, a more detailed study appears to be needed owing to the complexity of the mechanism of formation of geopolymers and the current availability of experimental data for model validation. By using the partial charge model (PCM) corroborated with experimental data, this paper attempts to elucidate the specific chemistry associated with the formation of low Si/Al geopolymer systems, generally referred to as poly(sialate) geopolymers. The study particularly includes dissolution and hydrolysis processes of aluminosilicate minerals, and the condensation reactions of aluminate and silicate species. The present study is based on metakaolin-based geopolymers, therefore, the speciation processes described here remain to be tested for geopolymers made from other aluminosilicate feedstock sources. However, the methodology and analysis presented are deemed applicable to geopolymer synthesis as a whole.

The formation of other high silicate derivatives, referred to as poly(sialate-siloxo) and poly(sialate-disiloxo) geopolymers, will be discussed in Part II of this paper since the variety of activators reported in the literature leads to different silicate species formation mechanisms.

#### Background to development of the partial charge model (PCM)

The partial charge model is based on Sanderson's "electronegativity equalization" assumption [17]. This principle also provides the basis of the discussion

presented in this study. By calculating the partial charge distribution in molecular species, Henry et al. [16] demonstrated that the chemical reactivity of metal ions during the processes of hydrolysis and condensation can be predicted and explained [18, 19]. For example, this model has been applied to explain the relative tendency toward hydrolysis behaviour of various alkoxides including  $\text{Ce}(\text{OPr}^i)_4$ ,  $\text{Zr}(\text{OPr}^i)_4$ ,  $\text{Ti}(\text{OPr}^i)_4$  and  $\text{Si}(\text{OPr}^i)_4$  among others [20], as experimental results have confirmed.

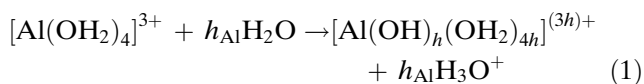
However, it is also evident that the model does not consider such factors as coordination number change before and after reaction, and the multivalent electron structure or lone pair electrons of atoms [19]. These parameters are known to have an important influence on chemical reactivity [21]. Nevertheless, for the elements of Al and Si in geopolymers, these effects are minor since there is no coordination number change before and after hydrolysis and condensation reactions in geopolymer synthesis, and Al and Si atoms only show univalent behaviour. In principle, the values of partial charges calculated from the model are meaningful only when they are used for direct comparisons, since the method of calculation and associated partial charge values are different for different electronegativity systems (i.e. Pauling's electronegativity, Mulliken–Jaffe's electronegativity, etc.) [19, 21].

Other sophisticated models have also been developed to calculate the partial charge distributions of zeolite molecular species, although these have produced some conflicting results [22, 23]. Hence to this point, experimental evidence provides the only basis for model validation.

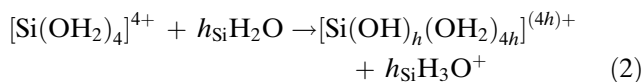
#### Model of dissolution, hydrolysis and condensation of geopolymer formation under highly alkaline conditions by the PCM

Mechanism of dissolution of metakaolin and hydrolysis of  $\text{Al}^{3+}$  and  $\text{Si}^{4+}$  ions under alkaline conditions

The initial formation of geopolymers involves the dissolution of metakaolin, which provide aluminate ions and, at least, part of the silicate components required for geopolymer synthesis. The hydrolysis reactions between the dissolved  $\text{Al}^{3+}$  and  $\text{Si}^{4+}$  ions and water probably occur simultaneously with the dissolution process. Considering that the coordination number of both  $\text{Al}^{3+}$  and  $\text{Si}^{4+}$  ions is 4 [24], the hydrolysis process of  $\text{Al}^{3+}$  and  $\text{Si}^{4+}$  ions in geopolymer systems may occur as follows [18]:

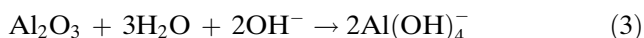


where  $h_{\text{Al}}$  is the hydrolysis ratio of  $\text{Al}^{3+}$ , and



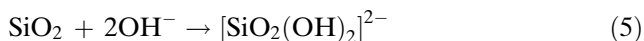
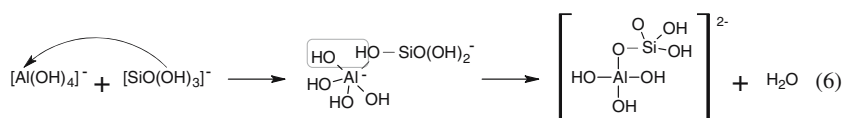
where  $h_{\text{Si}}$  is the hydrolysis ratio of  $\text{Si}^{4+}$ .

It has previously been shown that the hydrolysis ratio and possible resultant Al and Si species in alkaline conditions can be predicted by adopting the PCM [15]. Based on the PCM, the calculated results indicate that the major Al species under alkaline conditions is  $[\text{Al}(\text{OH})_4]^-$ , while the major silicate species are  $[\text{SiO}(\text{OH})_3]^-$  and  $[\text{SiO}_2(\text{OH})_2]^{2-}$ , with the concentration ratio of  $[\text{SiO}_2(\text{OH})_2]^{2-}$  to  $[\text{SiO}(\text{OH})_3]^-$  increasing with pH value. Therefore, the dissolution and hydrolysis of aluminosilicate mineral raw materials in alkaline conditions can be schematically expressed by the following reactions, if only mass and charge balances are considered:



In geopolymer synthesis, two kinds of activator are typically used—either straight alkaline hydroxide solutions or a blend of alkaline silicate solutions with alkaline hydroxide. Alkaline silicate solutions with alkaline hydroxide are usually used for producing geopolymers referred to as poly(sialate-siloxo) and poly(sialate-disiloxo). The difference between these two activators is that the first is of very low silicate content, while the silicate content in the second activator is high. The resulting silicate speciation will be different [29], consequently geopolymers made from different activators can be different in structure and properties, since the condensation reaction is dependent on the speciation of aluminate and silicate species. However, only the formation mechanism of geopolymers produced from low silicate activators is discussed in this paper.

This type of condensation reaction is usually a nucleophilic substitution reaction. For example, schematically, the condensation reaction between  $[\text{Al}(\text{OH})_4]^-$  and  $[\text{SiO}(\text{OH})_3]^-$  species may be expressed by the following reaction:



These reactions suggest that  $\text{H}_2\text{O}$  molecules and  $\text{OH}^-$  ions are consumed with continuous dissolution.

#### Mechanism of aluminate-silicate condensation

It has been well established [5] that the setting and hardening of geopolymers occur as a result of condensation between aluminate and silicate species. Similar condensation reactions also occur during zeolite synthesis [25, 26]. Moreover, experimental results [15, 27, 28] in the literature have shown that the condensation between aluminate and silicate species occur much more rapidly than that between silicate species themselves, but the mechanisms involved are not fully clear.

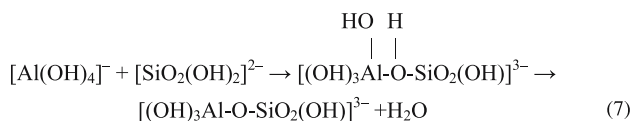
In reaction (6),  $[\text{Al}(\text{OH})_4]^-$  and  $[\text{SiO}(\text{OH})_3]^-$  species are linked to each other by the attraction between one of the OH groups from  $[\text{SiO}(\text{OH})_3]^-$  and Al ion of  $[\text{Al}(\text{OH})_4]^-$ , which results in an intermediate complex. The two OH groups in the intermediate complex then condense to form an aluminosilicate species by releasing a  $\text{H}_2\text{O}$  molecule. According to the PCM, the probable reaction paths and stability of resulting species may be determined by the following rules [15]:

- The partial charges of metal atoms ( $\delta_{\text{M}}$ ) in reactant species must be positive, while those of OH groups ( $\delta_{\text{OH}}$ ) from reactant species must be negative, to ensure that the species attract each other, leading to the occurrence of a condensation reaction.
- Additionally, the occurrence of condensation reactions also depends on the stability of the resultant species. Thus, the respective partial charge of metal

atoms and hydrogen atoms of species in the resulting product must be positive, while that of oxygen atoms remain negative.

- (c) The preferred reaction should have the larger absolute value of the product of the partial charges of metal atoms ( $\delta_M$ ) and OH groups ( $\delta_{OH}$ ) from the different reactants, i.e.,  $|\delta_M \times \delta_{OH}|$ , and consistent with (1) and (2) above.

According to our previous calculation [15],  $[\text{Al}(\text{OH})_4]^-$ ,  $[\text{SiO}_2(\text{OH})_2]^{2-}$  and  $[\text{SiO}(\text{OH})_3]^-$  species could exist under highly alkaline conditions.  $[\text{SiO}_2(\text{OH})_2]^{2-}$  species tend to be monomeric according to the partial charge distribution calculation, therefore the condensation between monomeric  $[\text{Al}(\text{OH})_4]^-$  and  $[\text{SiO}_2(\text{OH})_2]^{2-}$  may occur by the following reaction:

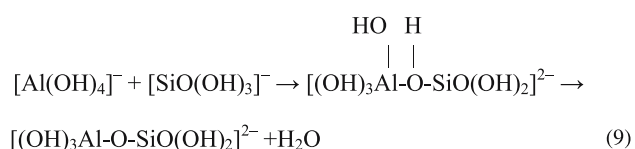


The calculated partial charges of the species in reaction (7) are shown in Table 1, which suggests that reaction (7) can take place without difficulty since the value of  $|\delta_{\text{Al}} \times \delta_{\text{OH}}|$  is large i.e., 0.27 (column 8; row 2), relative to other calculated values. Further condensation between the product of reaction (7) and  $[\text{Al}(\text{OH})_4]^-$  can occur, but the condensation between the product of reaction (7) and  $[\text{SiO}_2(\text{OH})_2]^{2-}$  is not preferred because the resultant product  $[\text{Al}(\text{OH})_2\text{-Si}_2\text{O}_6(\text{OH})_4]^{5-}$  has a negatively charged H atom next to a negatively charged O atom (Table 1), implying that the product may not be stable. Table 1 suggests that dimeric and trimeric aluminosilicate species may be dominant under the conditions of very high alkalinity, but the occurrence of higher polymerisation of aluminosilicates necessary to form and harden geopolymer is difficult under such high pH conditions.

With lowering alkalinity in activators,  $[\text{SiO}(\text{OH})_3]^-$  species become dominant according to the following reaction:



The condensation between  $[\text{Al}(\text{OH})_4]^-$  and  $[\text{SiO}(\text{OH})_3]^-$  may happen, as shown in reaction (9):



According to the calculated results (Table 2), the condensation between  $[\text{Al}(\text{OH})_4]^-$  and  $[\text{SiO}(\text{OH})_3]^-$  occurs favourably, moreover further condensation between the product of reaction (9) and  $[\text{SiO}(\text{OH})_3]^-$  can also occur to give stable products until all hydroxyl groups of  $[\text{Al}(\text{OH})_4]^-$  are consumed, consequently the polymeric aluminosilicate network begins to build up.

On the other hand,  $[\text{Al}(\text{OH})_4]^-$  species may also condense with both  $[\text{SiO}_2(\text{OH})_2]^{2-}$  and  $[\text{SiO}(\text{OH})_3]^-$  species, as shown in Table 3. For example,  $[\text{Al}(\text{OH})_2\text{-Si}_2\text{O}_5(\text{OH})_3]^{4-}$  species can be stable. However, the partial charge distribution suggests that the condensation between  $[\text{Al}(\text{OH})_4]^-$  and  $[\text{SiO}(\text{OH})_3]^-$  leads to more stable products. By contrast,  $[\text{Al}(\text{OH})_4]^-$  condensed with more than two  $[\text{SiO}_2(\text{OH})_2]^{2-}$  groups may produce unstable products.

In summary, the condensation between aluminate and silicate species is dependent on the speciation of silicate species based on the calculations shown in Tables 1–3. The condensation between  $[\text{Al}(\text{OH})_4]^-$  and  $[\text{SiO}_2(\text{OH})_2]^{2-}$  tends to form small oligomers, such as dimers and trimers, while the condensation between  $[\text{Al}(\text{OH})_4]^-$  and  $[\text{SiO}(\text{OH})_3]^-$  results in larger oligomers and polymers. Therefore, the formation of a geopolymer network relies on the concentration of  $[\text{SiO}(\text{OH})_3]^-$ . The relative concentration of  $[\text{SiO}_2(\text{OH})_2]^{2-}$  and  $[\text{SiO}(\text{OH})_3]^-$  species is determined by the alkalinity of the liquid phase during geopolymer synthesis, suggesting that alkalinity of the liquid phase of geopolymeric systems has an important influence on the condensation process.

## Experimental

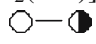
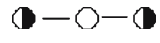

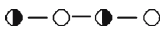
### Calorimetric measurement



For these experiments, 2.0 g metakaolin was mixed with 3.0 ml NaOH solutions with the concentrations of 1.0, 5.0, 10.0, and 15.0 M, respectively for five minutes before the calorimetric measurements started at 23 °C.

### Chemical analysis

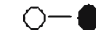
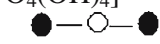
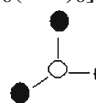
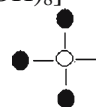
The dissolution rates of metakaolin in NaOH solutions were measured by reacting 20 g metakaolin with 30 mL of 2.0, 5.0 and 8.0 M NaOH solutions for 2, 10 and 60 min respectively, at room temperature before the liquors were separated from the solids by filtration under reduced pressure. The Al and Si compositions of the liquors were analysed by inductively coupled plasma optical emission spectroscopy.


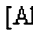
**Table 1** Partial charge change of  $\delta_x$  (where  $x = \text{Si, Al, H, O}$  and  $\text{OH}$ ) in reactant and resultant species in the condensation between  $[\text{SiO}_2(\text{OH})_2]^{2-}$  and  $[\text{Al}(\text{OH})_4]^-$

Reactant species	Resultant product*	$\Delta_{\text{Si}}$	$\delta_{\text{Al}}$	$\delta_{\text{H}}$	$\delta_{\text{O}}$	$\delta_{\text{OH}}$	$ \delta_{\text{Al}} \times \delta_{\text{OH}} $	Stability of product
$[\text{SiO}_2(\text{OH})_2]^{2-}$ + $[\text{Al}(\text{OH})_4]^-$	$[(\text{OH})_3\text{Al-O-SiO}_2(\text{OH})]^{3-}$ 	0.20		0	-0.55	-0.55	0.27	Stable
		0.23	0.49	0.09	-0.48	-0.39		
$[(\text{OH})_3\text{Al-O-SiO}_2(\text{OH})]^{3-}$ + $[\text{SiO}_2(\text{OH})_2]^{2-}$	$[\text{Al}(\text{OH})_2\text{Si}_2\text{O}_6(\text{OH})_2]^{5-}$ 	0.23	0.41	0.03	-0.53	-0.50	0.23	Unstable
		0.20		0	-0.55	-0.55		
		0.18	0.36	-0.02	-0.56	-		
$[(\text{OH})_3\text{Al-O-SiO}_2(\text{OH})]^{3-}$ + $[\text{Al}(\text{OH})_4]^-$	$[\text{Al}_2(\text{OH})_6\text{SiO}_4]^{4-}$ 	0.23	0.41	0.03	-0.53	-0.50	0.25	Stable
			0.49	0.09	-0.48	-0.39		
		0.23	0.42	0.03	-0.53	-0.50		
$[\text{Al}_2(\text{OH})_6\text{SiO}_4]^{4-}$ + $[\text{SiO}_2(\text{OH})_2]^{2-}$	$[\text{Al}_2(\text{OH})_6\text{Si}_2\text{O}_6]^{6-}$ 	0.23	0.42	0.03	-0.53	-0.50	0.23	Unstable
		0.20		0	-0.55	-0.55		
		0.17	0.35	-0.03	-0.57	-		

\*   $[\text{SiO}_2(\text{OH})_2]^{2-}$    $[\text{Al}(\text{OH})_4]^-$

**Table 2** Partial charge change of  $\delta_x$  (where  $x = \text{Si, Al, H, O}$  and  $\text{OH}$ ) in reactant and resultant species in the condensation between  $[\text{SiO}(\text{OH})_3]^-$  and  $[\text{Al}(\text{OH})_4]^-$

Reactant species	Resultant product*	$\delta_{\text{Si}}$	$\delta_{\text{Al}}$	$\delta_{\text{H}}$	$\delta_{\text{O}}$	$\delta_{\text{OH}}$	$ \delta_{\text{Al}} \times \delta_{\text{OH}} $	Stability of product
$[\text{SiO}(\text{OH})_3]^-$ + $[\text{Al}(\text{OH})_4]^-$	$[(\text{OH})_3\text{Al-O-SiO}(\text{OH})_2]^{2-}$ 	0.35		0.14	-0.44	-0.30	0.15	Stable
		0.31	0.49	0.09	-0.48	-0.39		
$[(\text{OH})_3\text{Al-O-SiO}(\text{OH})_2]^{2-}$ + $[\text{SiO}(\text{OH})_3]^-$	$[\text{Al}(\text{OH})_2\text{Si}_2\text{O}_4(\text{OH})_4]^{3-}$ 	0.31	0.50	0.10	-0.47	-0.37	0.15	Stable
		0.35		0.14	-0.44	-0.30		
		0.31	0.50	0.10	-0.47	-0.37		
$[\text{Al}(\text{OH})_2\text{Si}_2\text{O}_4(\text{OH})_4]^{3-}$ + $[\text{SiO}(\text{OH})_3]^-$	$[\text{Al}(\text{OH})\text{Si}_3\text{O}_6(\text{OH})_6]^{4-}$ 	0.31	0.50	0.10	-0.47	-0.37	0.15	Stable
		0.35		0.14	-0.44	-0.30		
		0.31	0.50	0.10	-0.47	-0.37		
$[\text{Al}(\text{OH})\text{Si}_3\text{O}_6(\text{OH})_6]^{4-}$ + $[\text{SiO}(\text{OH})_3]^-$	$[\text{AlO}_4\text{Si}_4\text{O}_4(\text{OH})_8]^{5-}$ 	0.31	0.50	0.10	-0.47	-0.37	0.15	Stable
		0.35		0.14	-0.44	-0.30		
		0.31	0.50	0.10	-0.47	-0.37		

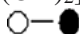
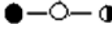
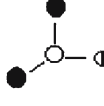
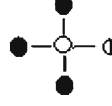
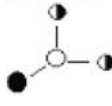
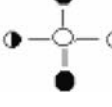
\*   $[\text{SiO}(\text{OH})_3]^-$    $[\text{Al}(\text{OH})_4]^-$

Low-resolution analytical NMR measurement

For these experiments, 2.0 g metakaolin was mixed with 3.0 mL of water and 1.0, 5.0, 10.0 and 15.0 M

NaOH solutions respectively at room temperature. To investigate the change of free water content during dissolution, hydrolysis and condensation processes, low-resolution analytical NMR measurements (Mini-

**Table 3** Partial charge change of  $\delta_x$  (where  $x = \text{Si}, \text{Al}, \text{H}, \text{O}$  and  $\text{OH}$ ) in reactant and resultant species in the condensation among  $[\text{SiO}_2(\text{OH})]^{2-}$ ,  $[\text{SiO}(\text{OH})_3]^{-}$  and  $[\text{Al}(\text{OH})_4]^{-}$ 

Reactant species	Resultant product	$\delta_{\text{Si}}$	$\delta_{\text{Al}}$	$\delta_{\text{H}}$	$\delta_{\text{O}}$	$\delta_{\text{OH}}$	$ \delta_{\text{Al}} \times \delta_{\text{OH}} $	Stability of product
$[\text{SiO}(\text{OH})_3]^{-} + [\text{Al}(\text{OH})_4]^{-}$	$[(\text{OH})_3\text{Al}-\text{O}-\text{SiO}(\text{OH})_2]^{2-}$ 	0.35 0.31	0.49 0.50	0.14 0.10	-0.44 -0.47	-0.30 -0.37	0.15	Stable
$[(\text{OH})_3\text{Al}-\text{O}-\text{SiO}(\text{OH})_2]^{2-} + [\text{SiO}_2(\text{OH})_2]^{2-}$	$[\text{Al}(\text{OH})_2\text{Si}_2\text{O}_4(\text{OH})_3]^{4-}$ 	0.31 0.20 0.21	0.50 0.39	0.10 0	-0.47 -0.55 -0.54	-0.37 -0.55 -0.53	0.28	Stable
$[\text{Al}(\text{OH})_2\text{Si}_2\text{O}_4(\text{OH})_3]^{4-} + [\text{SiO}(\text{OH})_3]^{-}$	$[\text{Al}(\text{OH})\text{Si}_3\text{O}_6(\text{OH})_5]^{5-}$ 	0.21 0.35 0.23	0.39 0.42	0.01 0.14 0.03	-0.54 -0.44 -0.53	-0.53 -0.30 -0.50	0.11	Stable
$[\text{Al}(\text{OH})\text{Si}_3\text{O}_6(\text{OH})_5]^{5-} + [\text{SiO}(\text{OH})_3]^{-}$	$[\text{AlO}_4\text{Si}_4\text{O}_4(\text{OH})_7]^{6-}$ 	0.23 0.35 0.25	0.42 0.44	0.03 0.14 0.05	-0.53 -0.44 -0.51	-0.50 -0.30 -0.46	0.15	Stable
$[\text{Al}(\text{OH})_2\text{Si}_2\text{O}_4(\text{OH})_3]^{4-} + [\text{SiO}_2(\text{OH})_2]^{2-}$	$[\text{Al}(\text{OH})\text{Si}_3\text{O}_7(\text{OH})_4]^{6-}$ 	0.21 0.20 0.18	0.39 0.36	0.01 0	-0.54 -0.55 -0.57	-0.53 -0.55 -	0.21	Unstable
$[\text{Al}(\text{OH})\text{Si}_3\text{O}_6(\text{OH})_5]^{5-} + [\text{SiO}_2(\text{OH})_2]^{2-}$	$[\text{AlO}_4\text{Si}_4\text{O}_5(\text{OH})_5]^{7-}$ 	0.23 0.20 0.21	0.42 0.39	0.03 0	-0.53 -0.55 -0.55	-0.50 -0.55 -0.54	0.13	Stable

spec, Bruker) were carried out on all samples. The relative content of free water in the samples was determined by analyzing the complete magnetization decay curve of the samples, governed by the “spin-spin” relaxation time  $T_2$  [30], which increases with increasing free water content in the samples.

#### MAS NMR measurements

Metakaolin and its mixtures with 5.0 M NaOH solutions for different durations were measured by NMR spectrometer. The  $^{27}\text{Al}$  and  $^{29}\text{Si}$  NMR spectra were

obtained using a Bruker Avance 400 spectrometer.  $^{27}\text{Al}$  and  $^{29}\text{Si}$  magic angle spinning (MAS) spectra were obtained by operating at 104.23 MHz for  $^{27}\text{Al}$  and 79.46 MHz for  $^{29}\text{Si}$ . The samples were loaded in 4 mm PSZ rotors with an accessible volume of 0.115 cm<sup>3</sup>, and rotation frequencies of 10 kHz and 12 kHz were used for the  $^{27}\text{Al}$  (400 accumulations) and  $^{29}\text{Si}$  (1,800 accumulations) MAS spectra respectively with a delay time of two seconds for both isotopes. No proton decoupling was used. The chemical shifts were measured with respect to zero reference from  $\text{Al}(\text{H}_2\text{O})_6^{3+}$  for  $^{27}\text{Al}$  and tetramethyl silane (TMS) for  $^{29}\text{Si}$ .

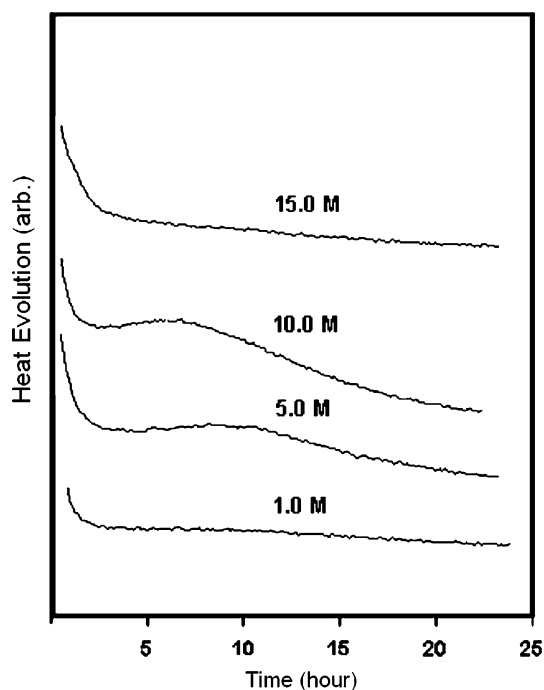
## Results

### Calorimetric measurement

The results of calorimetric measurement are shown in Fig. 1. The immediate large exothermic effect was observed when metakaolin was mixed with NaOH solutions within the range of 1.0–15.0 M. A second exothermic reaction occurred in the samples of 5.0 M and 10.0 M NaOH solution, with the exothermic event happening quicker and more pronounced in 10.0 M solution compared to the 5.0 M solution, as shown in Fig. 1.

### Chemical analysis

The concentration of Al and Si components from the dissolution of metakaolin in NaOH solutions are



**Fig. 1** Calorimetric results of the mixtures of metakaolin and NaOH solutions with 1.0, 5.0, 10.0 and 15.0 M concentration respectively

shown in Table 4. It was found that higher alkalinity resulted in higher dissolved Al and Si contents. For instance,  $[\text{Si}^{4+}]$  after 60 min of digestion is five times higher for the 8.0 M NaOH solution than for the 2.0 M solution. However, the digestion rate decreased at longer digesting times. Also, the aluminum component in metakaolin tended to dissolve more easily than the silicon component, except in very high alkaline conditions (e.g. 8.0 M NaOH solution).

### Low-resolution analytical NMR measurements

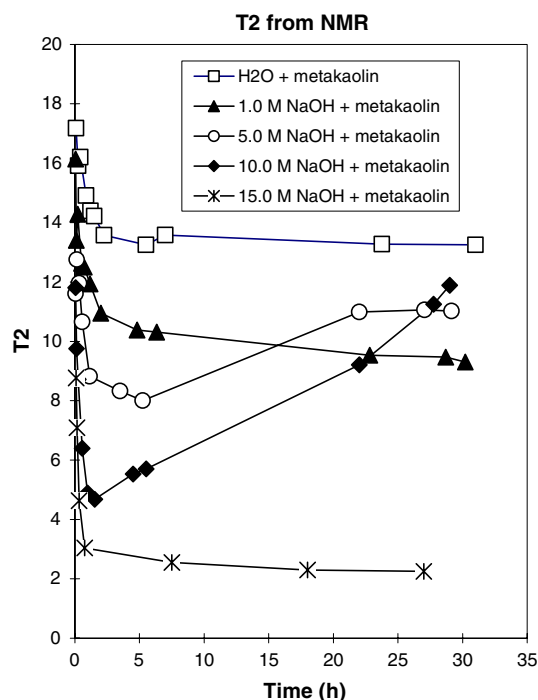
The relationship between relaxation time  $T_2$  and the reaction time in the samples with different alkalinity levels is given in Fig. 2.  $T_2$  decreased with reaction time within about 6 hours and thereafter remained stable for the reference metakaolin sample mixed with water. For the sample of metakaolin mixed with 1.0 M NaOH solution,  $T_2$  decreased within 2 h, thereafter, the rate of decrease diminished until the end of measurement (~30 h).  $T_2$  for the metakaolin sample mixed with 5.0 M NaOH solution decreased within 6 hours; increasing after that period until about 23 h, after which it remained stable to 30 h.  $T_2$  of the sample of metakaolin mixed with 10.0 M NaOH solution showed significant decrease in about 1.5 h, rising steadily thereafter until the end of measurement (30 h). The metakaolin sample mixed with 15.0 M NaOH solution showed a dramatic decrease of  $T_2$  within 1 h, followed by gradual decrease at a very slow rate.

### NMR measurements

There were two peaks at 28 ppm and 10 ppm with a shoulder at 58 ppm in the  $^{27}\text{Al}$  NMR spectrum of metakaolin, as shown in Fig. 3a, while the  $^{29}\text{Si}$  NMR spectrum of metakaolin showed a broad peak at  $-103$  ppm (Fig. 3b). After the metakaolin reaction with NaOH solution for 2 h, a new strong peak at 78 ppm appeared, and the shoulder at 58 ppm became an identifiable peak in the  $^{27}\text{Al}$  NMR spectrum (Fig. 3a), while a shoulder around  $-87$  ppm emerged beside the peak at  $-103$  ppm in the  $^{29}\text{Si}$  NMR spectrum (Fig. 3b).

**Table 4** Chemical analysis of Al and Si concentration of extracts from metakaolin reaction with NaOH solutions

NaOH solution (M)	Al concentration (M)			Si concentration (M)		
	2 min	10 min	60 min	2 min	10 min	60 min
2.0	0.040	0.071	0.077	0.019	0.055	0.050
5.0	0.067	0.133	0.173	0.037	0.103	0.144
8.0	0.088	0.189	0.268	0.050	0.154	0.278



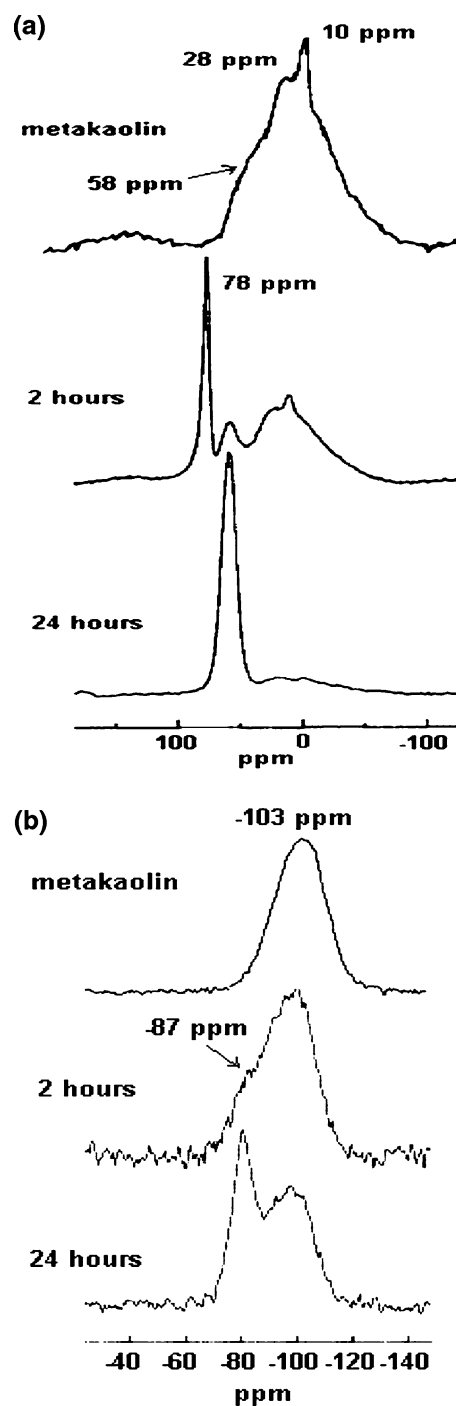
**Fig. 2** The relationship between spin–spin relaxation time  $T_2$  of the samples of metakaolin reaction with different NaOH solutions and digestion time

With the extension of reaction duration to 24 h, the peak at 78 ppm disappeared. The corresponding peaks at 28 ppm and 10 ppm were greatly weakened to a small and broad hump, and the intensity of the peak at 58 ppm became very strong in the  $^{27}\text{Al}$  NMR spectrum. Meanwhile, the shoulder at  $-87$  ppm developed to a strong peak, while the intensity of the broad peak at  $-103$  ppm weakened in the  $^{29}\text{Si}$  NMR spectrum (Fig. 3b).

## Discussion

Dissolution of metakaolin and hydrolysis of  $\text{Al}^{3+}$  and  $\text{Si}^{4+}$  ions under alkaline conditions

According to the predictions of the PCM (Sect. “Mechanism of dissolution of metakaolin and hydrolysis of  $\text{Al}^{3+}$  and  $\text{Si}^{4+}$  ions under alkaline conditions”), the dissolution and hydrolysis of metakaolin under alkaline conditions generate  $[\text{Al}(\text{OH})_4]^-$ ,  $[\text{SiO}_2(\text{OH})_2]^{2-}$  and  $[\text{SiO}(\text{OH})_3]^-$  species. From the NMR results shown in Fig. 3, the dissolution and hydrolysis process at the early stages of geopolymer formation suggest a reaction path consistent with model predictions.



**Fig. 3** MAS NMR spectra of raw metakaolin and metakaolin reacted with 5.0 M NaOH solution at different times: (a)  $^{27}\text{Al}$  NMR; and (b)  $^{29}\text{Si}$  NMR

Essentially the two peaks at 28 ppm and 10 ppm in the  $^{27}\text{Al}$  NMR spectrum of metakaolin shown in Fig. 3a can be attributed to 5- and 6-coordinated Al atoms, while the shoulder at 58 ppm is assigned to 4-coordinated Al atoms with each atom being coordinated with 4 Si atoms in the secondary coordination



environment [6]. The peak at  $-103$  ppm in the  $^{29}\text{Si}$  NMR spectrum of metakaolin in Fig. 3b is due to 4-coordinated Si atoms with each atom secondarily coordinating with one Al atom. After metakaolin reacts with NaOH solution for 2 h, the new peak at 78 ppm in the  $^{27}\text{Al}$  NMR spectrum emerges due to the formation of free  $[\text{Al}(\text{OH})_4]^-$  species according to [31], while the appearance of the shoulder at  $-87$  ppm in the  $^{29}\text{Si}$  NMR spectrum suggests Si atoms partly formed new aluminosilicate species, with each Si atom coordinating with 4 Al atoms secondarily. These results indicate that the sample of metakaolin mixed with NaOH solution at the early stage (2 hours) consisted of undissolved metakaolin, free  $[\text{Al}(\text{OH})_4]^-$  species and a small amount of newly formed aluminate-silicate species.

The existence of free  $[\text{Al}(\text{OH})_4]^-$  species is consistent with the predictions of the PCM. However, no apparent existence of monomeric silicate species was observed in the NMR results. The absence of monomeric silicate species during dissolution may be due to their rapid condensation with  $[\text{Al}(\text{OH})_4]^-$  to generate aluminosilicate species, which is supported by the appearance of the shoulder at around  $-87$  ppm in the  $^{29}\text{Si}$  NMR spectra (Fig. 3b). This condensation reaction consumes most of the monomeric silicate species that may be present since the content of Al components in the liquid phase is higher than Si components according to the chemical analysis results (Table 4), and also relatively more reactive.

According to reactions (3)–(5), the dissolution and hydrolysis of metakaolin result in a decrease of free water. This prediction is consistent with the low-resolution NMR results (Fig. 2), in which a decrease of free water content within the first several hours in metakaolin samples mixed with NaOH was clearly evident, although the decrease in  $T_2$  in Fig. 2 is partly attributed to the absorption of water on the surface of metakaolin particles. Correspondingly, the first large exothermic peaks in the calorimetric results (Fig. 1) can be assigned to the dissolution process of metakaolin, similar to the findings of Alonso and Palomo [32] and Granizo and Blanco-Valera [33]. The calorimetric results further disclose that the dissolution process is initiated as soon as metakaolin is mixed with NaOH solutions. However, the digestion rate of metakaolin appears to be related to the alkalinity according to the chemical analysis results (Table 4), and consistent with reactions (3)–(5). Therefore, the alkalinity decreased with digestion time, probably due to the consumption of  $\text{OH}^-$  ions, and hence the decrease of concentration and corresponding increase of concentration of resultant species during the dissolution process.

### Condensation of aluminate-silicate species with extended reaction time

After metakaolin reacted with NaOH solution for 24 h, 5- and 6-coordinated Al atoms in the metakaolin appeared to change their coordination number to 4, while free  $[\text{Al}(\text{OH})_4]^-$  species disappeared as shown by the  $^{27}\text{Al}$  NMR results (Fig. 3(a)), suggesting that it was consumed by the condensation with silicate species, along with continuous dissolution and hydrolysis.

The corresponding increase of the spin-spin relaxation time  $T_2$  with curing time of some samples in Fig. 2 suggests an increase of water content. This latter observation provides some evidence of the occurrence of condensation reactions (e.g., reaction (6)) in the samples. However, such condensation was only observed under a certain alkalinity range, particularly 5.0–10.0 M NaOH solutions, according to Fig. 2. The low-resolution NMR results (Fig. 2) further suggests that the second exothermic peak in the calorimetric results shown in Fig. 1 are attributable to the condensation reaction, in accordance with other studies [34, 35]. Similarly, the calorimetric results disclose that the condensation reactions preferably occur under specific alkaline conditions. When the alkalinity of solutions is not high enough, i.e., 1.0 M NaOH solution, the dissolution rate of metakaolin is slow (Table 4), and the net concentration of the resultant species is too low for apparent condensation to occur. However, if the alkalinity is too high, most of the resultant silicate species may exist as  $[\text{SiO}_2(\text{OH})_2]^{2-}$ , which is not favoured for condensation processes, according to the PCM predictions detailed in Sect. “Mechanism of aluminate-silicate condensation”. Therefore, condensation reactions can only be observed within a certain alkalinity range, i.e., 5.0–10.0 M NaOH solutions, as shown in Fig. 1 and 2.

### Formation of poly(sialate) geopolymers and their possible properties

In view of the above discussions on the mechanism of dissolution, hydrolysis and condensation, the process of geopolymer formation under high alkaline and low Si content conditions appears to involve the following steps.

When an activator is added to metakaolin, the dissolution process starts immediately. The resultant species in the liquid phase are likely to be monomeric  $[\text{Al}(\text{OH})_4]^-$ ,  $[\text{SiO}_2(\text{OH})_2]^{2-}$  and  $[\text{SiO}(\text{OH})_3]^-$ , which subsequently condense with each other. It should be noted that the condensation between Al and Si species occurs more readily due to the characteristic high

activity of  $[\text{Al}(\text{OH})_4]^-$ . The activity of aluminate species is attributed to such factors as higher partial charge, larger atomic size and four hydroxyl groups [14]. For  $[\text{SiO}(\text{OH})_3]^-$  and  $[\text{SiO}_2(\text{OH})_2]^{2-}$ , although the latter species is more capable of condensing with  $[\text{Al}(\text{OH})_4]^-$  since there exists a larger attraction, they produce only small aluminosilicate oligomers. With a decrease of alkalinity in the activator, the concentration of  $[\text{SiO}(\text{OH})_3]^-$  species increases, resulting in further condensation between  $[\text{Al}(\text{OH})_4]^-$  and silicate species, which gives larger oligomers, leading to a gradual build up of aluminosilicate networks.

## Conclusions

For systems characterised by  $\text{Si}/\text{Al} \leq 1$ , solid-state NMR detection of monomeric  $[\text{Al}(\text{OH})_4]^-$  species after two hours of metakaolin dissolution in 5 M NaOH solution is consistent with predictions of the partial charge model. It is further noted that the absence of corresponding monomeric silicate species from NMR spectra for 5.0–10.0 M NaOH solution suggests possible rapid condensation with  $[\text{Al}(\text{OH})_4]^-$  to generate aluminosilicate species, as indicated by the evolution of the shoulder at around  $-87$  ppm in the  $^{29}\text{Si}$  NMR spectra. Of the two stable silicate species  $[\text{SiO}(\text{OH})_3]^-$  and  $[\text{SiO}_2(\text{OH})_2]^{2-}$ , the latter appears most likely to condense with  $[\text{Al}(\text{OH})_4]^-$  to produce small aluminosilicate oligomers, given its larger ionic charge density. Calorimetric and low-resolution NMR data further suggest that for systems with  $\text{Si}/\text{Al} \leq 1$ , the occurrence of condensation reactions appears to be favoured only within a certain alkalinity range, i.e., 5.0–10.0 M NaOH solutions. Overall, the outlined dissolution and hydrolysis process at the early stages of geopolymer synthesis suggest a reaction path consistent with the predictions of the partial charge model.

**Acknowledgments** The assistance of our colleagues Dr Iko Burgar and Dr Puyam Singh with solid-state NMR experiments is greatly appreciated.

## References

- Davidovits J (1982) US Patent 4349386
- Davidovits J, Orlinski J (eds) (1988) Proceedings of Geopolymer International Conference, Compiègne, France
- Davidovits J, Davidovits R, James C (eds) (1999) Proceedings of Geopolymer International Conference, Saint-Quentin, France. ISBN 2-902933-14-2
- Lukey G (ed) (2002) Proceedings of Geopolymer International Conference, Melbourne, Australia. ISBN 0-97502242-0-5
- Davidovits J, Davidovics M, Davidovits N (1994) US Patent 5342595
- Barbosa V, Mackenzie K, Thaumaturgo C (2000) *Int J Inorg Mater* 2:309
- Lowenstein W (1954) *Am Mineral* 39:92
- Provis JL, Duxson P, Lukey GC, Van Deventer JSJ (2005) *Chem Mater* 17(11):2976
- Palomo A, Glasser F (1992) *Br Ceram Trans J* 91:107
- Stevenson M, Sagoe-Crentsil K (2005) *J Mater Sci* 40:2023
- Davidovits J (1988) in Proceedings of geopolymer'88, p 25
- Rahier H, Van Mele B, Biesemans M, Wastiels J, Wu X (1996) *J Mater Sci* 31:71
- Rahier H, Simons W, Van Mele B, Wastiels J (1997) *J Mater Sci* 32:2237
- Xu H, Van Deventer JSJ (1999) in Proceedings of Geopolymer '99, Saint-Quentin, France, p 43
- Weng L, Sagoe-Crentsil K, Brown T, Song S (2005) *Mater Sci Eng B: Solid-State Mater Adv Technol* 117(2):163
- Henry M, Jolivet J, Livage J (1992) *J Struct Bond* 77:153
- Sanderson RT (1951) *Science* 114:670
- Livage J, Henry M (1988) In: Mackenzie JD, Ulrich DR (eds) *Ultrastructure processing of advanced ceramics*. John Wiley & Sons, New York, p 183
- Livage J, Henry M, Sanchez C (1988) In: *Sol-gel chemistry of transition metal oxides*. Progress in solid state chemistry, pp 259–341
- Livage J, Sanchez C (1992) *J Non-Cryst Solids* 145:11
- Huheey JE, Keiter EA, Keiter RL (1993) *Inorganic chemistry: principles of structure and reactivity*, 4th edn. Harper & Collins College Pub. Inc., New York
- Henry M, (2002) *Chem Phys Chem* 3:561
- de Jong BHWS, Brown GE (1980) *Geochimica et Cosmochimica Acta* 44(3):491
- Swaddle T (2001) *Coordinat Chem Rev* 219–221:665
- Zhdanov L (1968) *Molecular sieves*. Society of Chemical Industry, London, UK, p 62
- Barrer R (1982) *Hydrothermal chemistry of zeolites*. Academic Press, London, UK
- Glasser L, Lachowski E (1980) *J Chem Soc Dalton Trans* 3:393
- Glasser L, Harvey G (1984) *J Chem Soc Chem Commun* 16:1250
- Ray N, Plaisted R (1983) *J Chem Soc Dalton Trans* 3:475
- Barker P (1987) *Minispec applications note*. Bruker Optics Inc, MA USA, p 30
- Faust B, Labiosa W, Dai K, Macfall J, Browne B, Ribeiro A, Richter D (1995) *Geochimica et Cosmochimica Acta* 59:2651
- Alonso S, Palomo A (2001) *Mater Lett* 47:55
- Granizo ML, Blanco-Valera MT (1998) *J Thermal Anal* 52:957
- Robens E, Benzler B, Buchel G, Reichert H, Schumacher K (2002) *Cem Concr Res* 32:87
- Nocun-Wczelik W (2001) *J Thermal Anal Calorimet* 65:613